

# MODELING OF AMMONIA SOLUTION SPRAY AND MIXING IN SELECTIVE CATALYTIC REDUCTION (SCR) SYSTEM

Shijie Xu<sup>1\*</sup>, Xue-Song Bai<sup>1</sup>, Yaopeng Li<sup>1</sup>, Leilei Xu<sup>1,2</sup>, Peter Larsson<sup>1</sup>, Per Tunestål<sup>1</sup>

<sup>1</sup> Department of Energy Sciences, Lund University, 22100 Lund, Sweden

<sup>2</sup> Key Lab. for Power Machinery and Engineering of M.O.E., Shanghai Jiao Tong University, Shanghai, P.R. China

## ABSTRACT

In this work, numerical simulation was carried out to study the injection and mixing of ammonia solution spray in the exhaust pipe of diesel engines. The ammonia solution was injected into the hot gas of 623 K. The spray was vaporized into gas and mixed with the hot exhaust gas and together the mixture was transported in the exhaust gas pipe downstream where a selective catalytic reduction (SCR) system was implemented to convert NO<sub>x</sub> to H<sub>2</sub>O and N<sub>2</sub>. The effects of exhaust pipe geometry and gravity on the droplet evolution and vapor mass fraction were investigated. The results show that the influence of gravity is negligible, while the exhaust pipe geometry has a great impact on the vapor distribution. In straight pipe case the NO<sub>x</sub> reduction is only achievable in a small area of the catalyzer, which is in good agreement with the experiments. Analysis of the velocity field and streamlines shows that the ammonia vapor is blocked by a recirculation zone; as a result, the vapor mass fraction will be centralized into a small zone because radial component of vapor velocity is too slow to penetrate into the center of main flow. In addition, the spray droplet size distribution indicates that a certain amount of ammonia enters into catalyzer as liquid phase with medium diameter around 19 and 17 μm in straight and bending pipe, which further deteriorates the catalytic efficiency. The results provide a guidance for the design of ammonia injector and the exhaust pipe geometry.

**Keywords:** exhaust gas after treatment, selective catalytic reduction, ammonia

## 1. INTRODUCTION

As one of the most important emissions in diesel engine combustion, nitric oxide (NO<sub>x</sub>) plays an important

role in air pollution, causing a series of atmospheric problems, such as toxic gas, acid rain and photochemical pollution. Selective Catalytic Reduction (SCR) is a promising exhaust after treatment technology, which has been shown to achieve 90% NO<sub>x</sub> reduction in diesel engine exhaust gas [1]. In SCR system, adblue (urea water solution) is injected in engine exhaust pipe, vaporizes and mixes with high temperature exhaust gas in which urea decomposes into ammonia and converts NO<sub>x</sub> to H<sub>2</sub>O and N<sub>2</sub> in the following catalyst chamber [2]. To achieve a high catalyzer conversion efficiency, a uniform ammonia distribution at catalyzer inlet is desired [3]. The distribution is related to the arrangement of SCR system, including injector location and exhaust pipe geometry. Investigation of spray in SCR system has been conducted both in numerical simulation [4][5] and experimental studies [6][7]. Recently, our cooperative group conducted a series of experiments [8][9] on ammonia solution spray in SCR system, focusing on droplet distribution and the optimization of exhaust pipe geometry. Larsson et al. [9] found that bent pipe configuration performs better in terms of NO<sub>x</sub> conversion efficiency.

In this work, numerical simulation was carried out based on Larsson et al. [9] experimental setups to provide interpretation on the influence of exhaust pipe geometry. The effects of pipe geometry and gravity on the droplet evolution and vapor mass fraction were investigated. The main objectives of this work are to: (1) demonstrate the effect of gravity, which is essential for the design of SCR system installation direction, (2) investigate the droplet size evolution and vapor distribution and under two different lengths of mixing chamber, (3) compare the performance with respect to the conversion efficiency in bending and straight pipe.

## 2. METHODOLOGY

An unsteady Reynolds-averaged Navier-Stokes approach (URANS) is employed to describe the compressible gas phase, with a standard k-epsilon model to compute the turbulence transport term. In addition, the liquid phase is modeled using the Lagrangian particle tracking (LPT) approach [10], in which a number of parcels are tracked to take the evaporating droplets into account. A Rosin-Rammler distribution is employed to describe the initial droplet size distribution, while the breakup process is modeled using Reitz-Diwakar model, which has been validated and shown a good performance in application of SCR urea-water solution spray simulation [5]. It is worth noting that, on one hand, the catalyst chamber is not included in the computational domain, only non-reacting flow with evaporation and mixing before catalyst chamber is considered. On the other hand, since the concentration of adblue in water solution is low, the physical properties of adblue-water solution is regarded as the same as pure water.

## 3. CASE SET-UP

### 3.1 Geometries

The basic geometry is a straight exhaust pipe with a cone for spray, the diameter of exhaust pipe is 60 mm. The bending pipe has the same diameter but a branch angle of 60 degrees. Fig. 1 shows the straight and bending pipes, respectively. The exhaust gas comes from the right side of pipe, mixes with the liquid injected from the cone, and then comes out in the left side and connect with the catalytic monolith by using an 80 mm length flared tube.

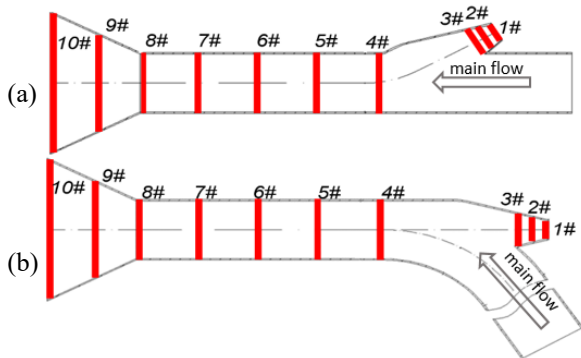


Fig 1 The pipe geometries: (a) straight pipe, (b) bending pipe. Red lines are probe sections for droplet size analysis.

Table 1 shows the numerical cases setups, Cases A-C are considered for grid sensitivity analysis, Cases C and D are studied to investigate the effect of gravity in the straight pipe. Case D and Case E, which are identical to

the experimental cases conducted in Ref. [9], are designed to study the geometry influence.

Table 1 Numerical case setups

Case	pipe geometry	grid quantity	gravity
A	straight	39816	With gravity
B	straight	501811	With gravity
C	straight	156194	With gravity
D	straight	156194	Without gravity
E	bending	199961	Without gravity

### 3.2 Boundary conditions

The boundary conditions are determined from experimental measurements in a metal engine with speed of 1500 rpm [9]. The exhaust gas is set with a mass flow of 145 kg/h and 623 K temperature. The adblue spray was injected at a mass flow is 0.8 kg/h with initial droplet velocity of 60 m/s, referring to measurement [8]. Of particular note is that the injection is intermittent, an injection cycle consists of 10 ms spray and an interval of 31 ms. To consider the interaction between two injections, multi-cycles are simulated to obtain a steady solution.

## 4. RESULTS AND DISCUSSIONS

### 4.1 Grid and gravity sensitive analysis

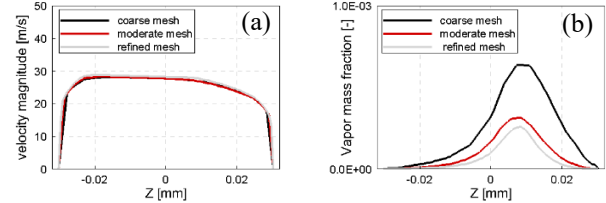


Fig 2 The grid sensitive analysis for Case A, B and C. (a) The velocity distribution at 10ms (b) the vapor mass fraction.

Cases A, B and C use coarse, refined and medium mesh with the same geometry and boundary conditions. A probe line along a radial-axis ( $Z$ ) is extracted in cross section 8# (cf. Fig.1, the numbered cross sections) between flared tube and exhaust pipe. Both velocity and vapor mass fraction distributions are employed for grid sensitive analysis. Fig.2(a) illustrates the axial velocity from the three cases, indicating that all grids show a satisfactory performance on velocity prediction. As for vapor mass fraction in Fig.2(b), all lines show a bell-shape, peaking around  $Z=8$  mm. However, a remarkable discrepancy between the results from the coarse and moderate mesh is observed in terms of the maximum value. By contrast, there is a small difference between moderate and refined mesh. In terms of sensitivity to gravity, the mass fraction distribution in Case C and D is the same

at the beginning, and the discrepancy is only identifiable at later stage, in the near the wall region. But even so, the overall distribution and local extremum resemble each other in Cases C and D. It can be concluded that, the gravity has no significant influence on the injection and mixing process. Therefore, it is reasonable to use moderate mesh without gravity as baseline case in the following analysis.

#### 4.2 Droplet evolution and distribution

Fig.3 shows the droplet statistics at different times. A sauter mean diameter (SMD) is applied to describe the average droplet diameter in each probe sections. The sections 1-10# are marked in Fig.1. At each section a thickness of 10 mm domain volume is taken for calculation of droplet statistics. It is found that liquid phase is not evaporated completely, the outlet droplet size is around 19 and 17  $\mu\text{m}$  in straight and bending pipe at 41 ms.

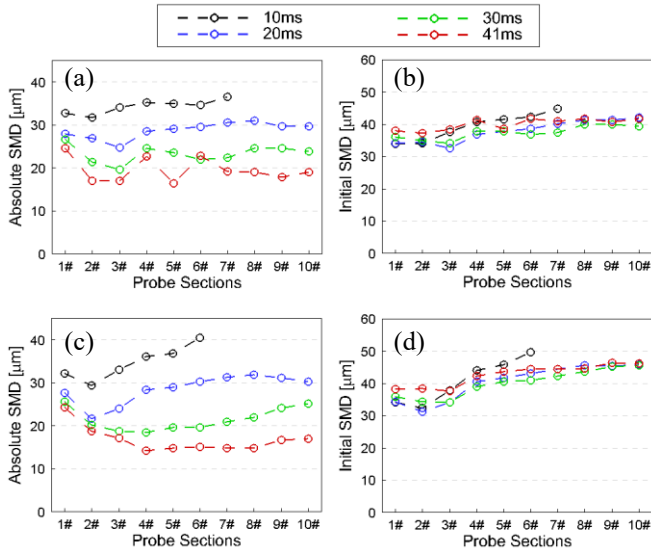


Fig. 3 The sauter mean diameter (SMD) evolution. (a)(b) represent the absolute diameter and initial diameter, probed in straight pipe; (c)(d) represent for bending pipe.

Of particular interest is that the SMD does not always decrease from upstream to downstream. This is more obvious in bending pipe, for instance, the average droplet diameter section in 6# is around 40  $\mu\text{m}$  at 10 ms which is evidently higher than in section 1#. The same phenomenon is observed in straight pipe. To explain it, both initial diameter and instantaneous diameter of each droplet are recorded. The initial value is the diameter when it is injected, it is invariable during evaporation and breakup. Figures (1b) and (2b) show the evolution of initial diameter in each spatial section; almost all lines coincide with each other and increase along with the main

flow stream. The droplet velocity after injection is significantly greater than the main flow, it will slow down after injection. However, because of low surface-volume ratio, it is difficult to slow down the droplets with larger diameter. Therefore, the droplet with larger diameter has a higher average speed and trends to be located in downstream.

Fig.4 illustrates the probability density function(PDF) of droplet size in section 6# at 10ms. As can be seen, the

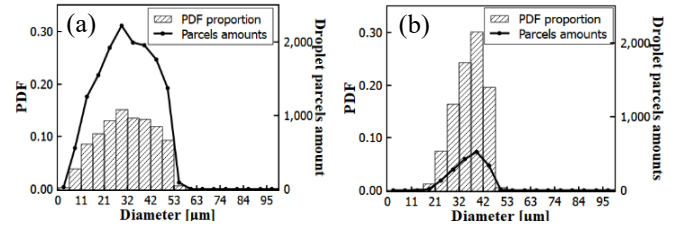


Fig 4 The droplet parcel amounts and size probability density distribution in straight pipe at 10ms,(a) section 1# and (b) section 6#.

PDF distributes in a narrow band in downstream, while the amounts of droplet parcels decrease. One possible reason is that the biggest particles break up into small one, while the small droplets decrease the diameter quickly because of evaporation. Since a large number of small droplets disappears, thus, the PDF of medium size particle increases, which results in a narrow band PDF around a medium size. Therefore, it is reasonable that the droplet SMD in downstream is larger than that in upstream in Fig.3.

Overall, in both straight and bending pipe, even though most of liquid phase is converted into vapor phase through breakup and evaporation, a significant amount of droplet with medium size does exist on the entrance of catalyzer chamber which will then reduce the catalyzer conversion efficiency.

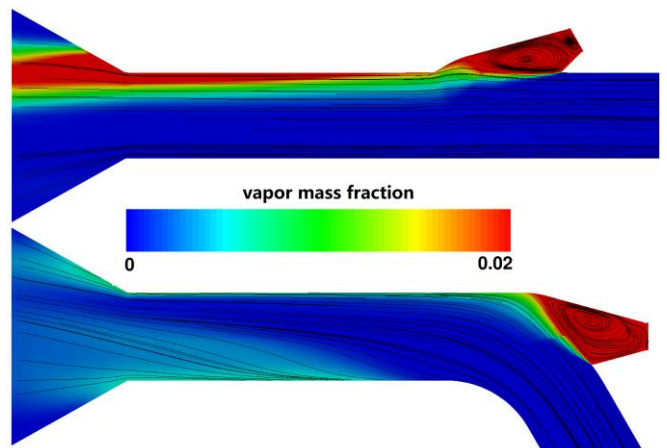


Fig 5. The streamlines in straight and bending pipe at 30ms, colored by vapor mass fraction.

Fig.5 demonstrates the vapor mass fraction and the streamline of the main flow on the outlet cross section at 30 ms. It is clear that the vapor mass fraction distribution in the bending pipe outlet section is more even than in the straight pipe. In this case the vapor in the spray cone is blocked by a recirculation zone, and the radial component of its velocity is too slow to penetrate into the center of main flow. As a consequence, the vapor mass fraction in the outlet of flared tube concentrates in a triangle-shape region in the upper side, spreading outward through a weak transportation and diffusion. In comparison, the vapor mass fraction distribution in bending pipe outlet section is more uniform due to the change of the mean flow. The spray cone axis is parallel to the main flow in the bending pipe, while the initial injection provides droplets a velocity component on the direction perpendicular to the main flow axis. This allows for a better mixing of the droplets and the flow and more uniform distribution in the pipe.

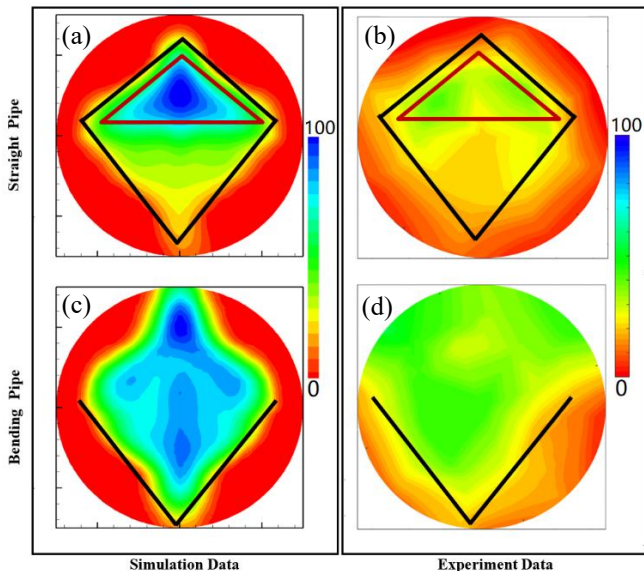


Fig 6 Accumulative vapor mass fraction and experimental catalytic efficiency data. (a) and (c) are numerical results of normalized vapor mass fraction in straight and bending pipes, while experimental catalytic efficiency in the corresponding pipes is shown in (b,c) [9].

In Fig.6, the vapor mass fraction in the outlet section is integrated within an injection cycle. It is clear that the vapor in the bending pipe is more widely distributed than the straight pipe, which forms a high concentration region in the upper part of the outlet section. Fig.6 also shows the experimental catalytic efficiency data. In comparison, the distribution of the simulation results and experiments is fairly similar. On one hand, the region with high ammonia concentration is seen in a triangle region in straight pipe, while in the bending pipe the region is

larger, resulting in a higher overall catalytic efficiency. On the other hand, both the straight and bending pipes show an unsatisfactory performance near the wall.

## 5. CONCLUSION

It has been found that a certain amount of ammonia enters into catalyzer as liquid phase with a medium diameter of 19 and 17  $\mu\text{m}$  in straight and bending pipe which deteriorates the catalytic efficiency. The gravity has no significant influence in terms of vapor distribution. As a consequence, this SCR system is able to be connected with the exhaust pipe without considering the installation direction.

The bending pipe has a better performance than the straight pipe on the vapor distribution. This is because that the ammonia vapor is blocked by a recirculation zone in both straight and bending pipe, while the radial component of vapor velocity in the straight pipe is too slow to penetrate into the center of main flow. As a result, the vapor mass fraction is centralized in a small zone, which leads to a low overall catalytic efficiency.

## ACKNOWLEDGEMENT

The authors would like to acknowledge the China Scholarship Council (CSC) and the Swedish biomimetics 3000 AB for financial support, and SNIC for computers.

## REFERENCE

- [1] Johnson TV. SAE International Journal of Engines. 2012;5(2):216-234.
- [2] Fritz A, Pitchon V. Applied Catalysis B: Environmental. 1997;13(1):1-25.
- [3] Sluder CS, Storey JM, Lewis SA, Lewis LA. SAE transactions. 2005:669-677.
- [4] Jeong SJ, Lee SJ, Kim WS. Environmental Engineering Science. 2008;25(7):1017-1036.
- [5] Shahariar GM, Lim OT. Energies. 2019;12(1):125.
- [6] Spiteri A, Eggenschwiler PD, Liao Y, Wigley G, Michalow-Mauke KA, Elsener M, Kröcher O, Boulouchos K. Fuel. 2015;161:269-77.
- [7] Grout S, Blaisot JB, Pajot K, Osbat G. Fuel. 2013;106:166-77.
- [8] Larsson P, Lennard W, Andersson O, Tunestål P. SAE Technical Paper. 2016. No. 2016-01-2211.
- [9] Larsson P, Ravenhill P, Larsson LU, Tunestål P. ASME 2018 ICE Division Fall Technical Conference. 2018. V002T04A005-V002T04A005.
- [10] Gong C, Jangi M, Bai XS. Applied energy. 2014;136:373-381.